# Commentary on manuscript "Comment on 'The one dimensional acoustic field with arbitrary mean axial temperature gradient and mean flow' (J. Li and A. S. Morgans, Journal of Sound and Vibration 400 (2017) 248-269)"

Jingxuan Li[a,b], Aimee S. Morgans[a,*]

[a]*Department of Mechanical Engineering, Imperial College London, South Kensington Campus, London SW7 2AZ, UK.*
[b]*School of Astronautics, Beihang University, Beijing 100191, China.*

---

## 1. Introduction and discussion

The authors sincerely thank Dukumaci for his great interest in our investigation. In his comment, he proposed an analytical solution based on the "matrizant" approach [1, 2]. The two linearised Euler equations as functions of pressure $\hat{p}$ and velocity perturbations $\hat{u}$ are transformed to a first order matrix ordinary differential equation (Eq. (3) in Dokumaci's comment) as functions of two new coefficients $p^{\pm}$ directly linking $\hat{p}$ and $\hat{u}$ (using Eq. (4) in his comment). At sufficiently high frequencies, the off-diagonal terms of the matrizant can be assumed zero; this decouples $p^{+}$ and $p^{-}$, and the analytical solution of $p^{\pm}$ (Eq. (7) in Dokumaci's comment) follows from the simplified first order matrix ordinary differential equation.

For consistency with our original paper [3]), key equations in Dokumaci's comment are rearranged. Using the mean property relations (Eqs. (5)-(11)in [3]), Eq. (7) in Dokumaci's comment becomes:

$$p^{\pm}(x) = C_1^{\pm}\mathcal{P}_1^{\pm}(x) \tag{1}$$

where the coefficients $\mathcal{P}_1^{\pm}(x)$ are expressed as:

$$\mathcal{P}_1^{\mp}(x) = \left(\frac{\bar{\rho}(x)}{\bar{\rho}(0)}\right)^{1/4} \exp\left(\int_0^x \left(\frac{\pm \mathrm{i}k_0}{1 \mp M} + \frac{\alpha}{2}\Big(\mp M\Big(1 + \frac{\gamma}{1 \mp M}\Big) + M^2\Big(\frac{\gamma}{2} - \frac{1}{1 \mp M}\Big)\Big)\right)\mathrm{d}x\right) \tag{2}$$

Time dependence $e^{\mathrm{i}\omega t}$ is assumed, following our previous treatment [3]. $\bar{\rho}$, $\alpha = \mathrm{d}(\ln\bar{\rho})/\mathrm{d}x$, $M$, $\gamma$, $k_0 = \omega/\bar{c}$ , $\omega$, $\bar{c}$ and $x$ are mean density, normalised first order differential of mean density, Mach number, ratio of specific heats, local wave number, complex angular frequency, speed of sound and axial location respectively. Note that the two coefficients $\mathcal{P}_1^{\pm}(0)$ equal 1 at the inlet ($x = 0$) of the duct with a mean temperature distribution. $C_1^{\pm}$ are two arbitrary coefficients which can be determined for given initial or boundary conditions. In Dokumaci's comment, $\hat{p}$ and $\hat{u}$ can be reconstructed using the following relations:

$$\hat{p}(x) = p^{+}(x) + p^{-}(x) = C_1^{+}\mathcal{P}_1^{+}(x) + C_1^{-}\mathcal{P}_1^{-}(x) \tag{3}$$

$$\hat{u}(x) = \frac{p^{+}(x) - p^{-}(x)}{\bar{\rho}\bar{c}} = \frac{1}{\bar{\rho}\bar{c}}\left(C_1^{+}\mathcal{P}_1^{+}(x) - C_1^{-}\mathcal{P}_1^{-}(x)\right) \tag{4}$$

In our work [3], a two-step procedure was used to obtain the analytical solution of the acoustic field: (1) firstly, an acoustic wave equation as a function of $\hat{p}$ (e.g., Eq. (27) in [3]) was derived based on linearised Euler equations; (2) the WKB approach was then applied to obtain analytical solutions. Assumptions were made and Mach number

*Corresponding author.
*Email addresses:* jingxuan.li@imperial.ac.uk,ljx.buaa@gmail.com (Jingxuan Li), a.morgans@imperial.ac.uk (Aimee S. Morgans)

terms with order exceeding $M^2$ were neglected in both steps, leading to a frequency criterion of [3]: $|k_0| \gg |\alpha|$ and $|k_0^2| \gg |\beta|/2$, where $\beta$ is the normalised second order differential of mean density. The "matrizant" approach of Dukumaci's comment is a one-step procedure whose only assumption is to neglect the off-diagonal terms of the matrizant. Mach number terms with higher orders are retained in the diagonal terms, extending applicability of the solution to large Mach numbers when the frequency is sufficiently large.

However, Dokumaci's decoupling criterion (which is equivalent to a frequency criterion) is derived based on equations which neglect mean flow contributions. To the authors' knowledge, this criterion then becomes invalid at larger Mach numbers. As the criterion in [3] was derived accounting for mean flow, it does not rigorously follow that Dokumaci's criterion is tighter than ours.

We examine the performance of the analytical simulations given by Dokumaci's comment and our previous work [3] by applying them to a straight duct containing one-dimensional mean flow, and with a distributed mean temperature zone extending from $x = x_1$ to $x = x_2 = x_1 + l$. Initially, a linearly decreasing temperature profile is considered. More detail on the duct configuration and temperature profile is given in [3].

Figures 1-3 show the predicted gain and phase of the acoustic transfer functions $\mathcal{F}_p$ and $\mathcal{F}_u$ (Eqs. (56) and (57) in [3]) against axial distance for two different flow Mach numbers and frequencies. Predictions using our previous analytical solution shows excellent agreement with the solution calculated using the two linearised Euler equations (Eqs. (16) and (19) in [3]), while predictions using Dokumaci's solution exhibit inaccuracies.

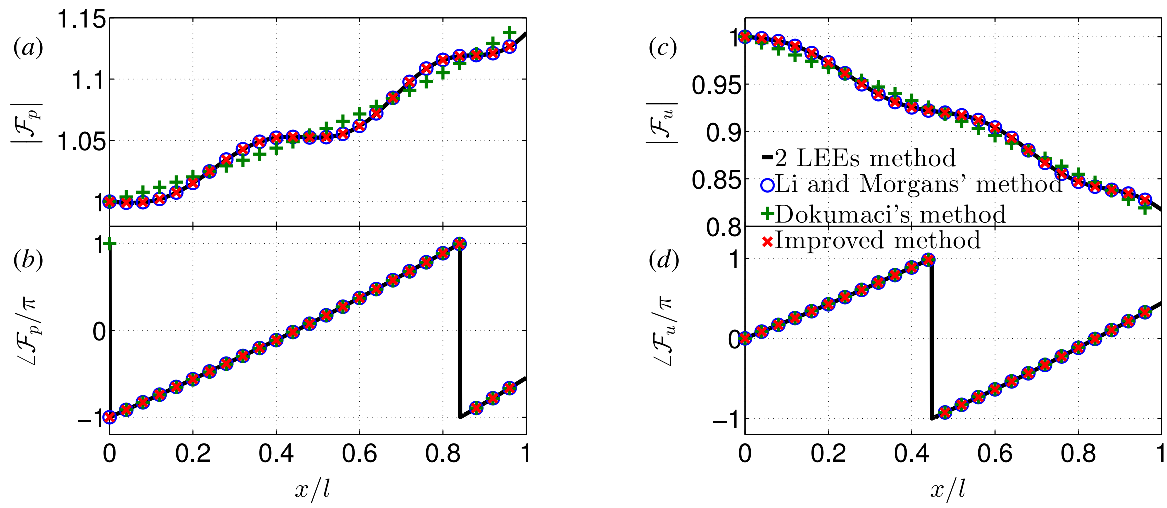


Figure 1: Evolution of $\mathcal{F}_p$ and $\mathcal{F}_u$ with $x$ for the linear mean temperature profile. $\overline{T}_1 = 1600$ K, $\overline{T}_2 = 800$ K, $M_1 = 0.05$, $fl/\bar{c}_1 = 1$ and $Z_1 = -1$. (a): transfer function gain $|\mathcal{F}_p|$. (b): transfer function phase $\angle\mathcal{F}_p$. (c): transfer function gain $|\mathcal{F}_u|$. (d): transfer function phase $\angle\mathcal{F}_u$.

## 2. Improved solution

Figures 1-3 demonstrate that, in the presence of a mean flow, the best performance of Dokumaci's solution occurs when the frequency is large. This observation has allowed the present authors to propose an improved solution. By substituting the analytical solution of $\hat{p}$ (Eq. (3)) into the linearised Euler equations (e.g., Eqs. (24) and (25) in [3]) and using the procedure (Eq. (46) in [3]), another version of the analytical solution of $\hat{u}$ is given by:

$$\begin{aligned}\hat{u}(x) = &\left(\frac{\mathrm{i}k_0 - \left(1 + 2(1+\gamma)M + (3\gamma - 7)M^2\right)\alpha/4}{\mathrm{i}k_0 - \alpha M}\right)\frac{C_1^+\mathcal{P}_1^+(x)}{\bar{\rho}\bar{c}} \\ &-\left(\frac{\mathrm{i}k_0 + \left(1 - 2(1+\gamma)M + (3\gamma - 7)M^2\right)\alpha/4}{\mathrm{i}k_0 - \alpha M}\right)\frac{C_1^-\mathcal{P}_1^-(x)}{\bar{\rho}\bar{c}}\end{aligned} \tag{5}$$

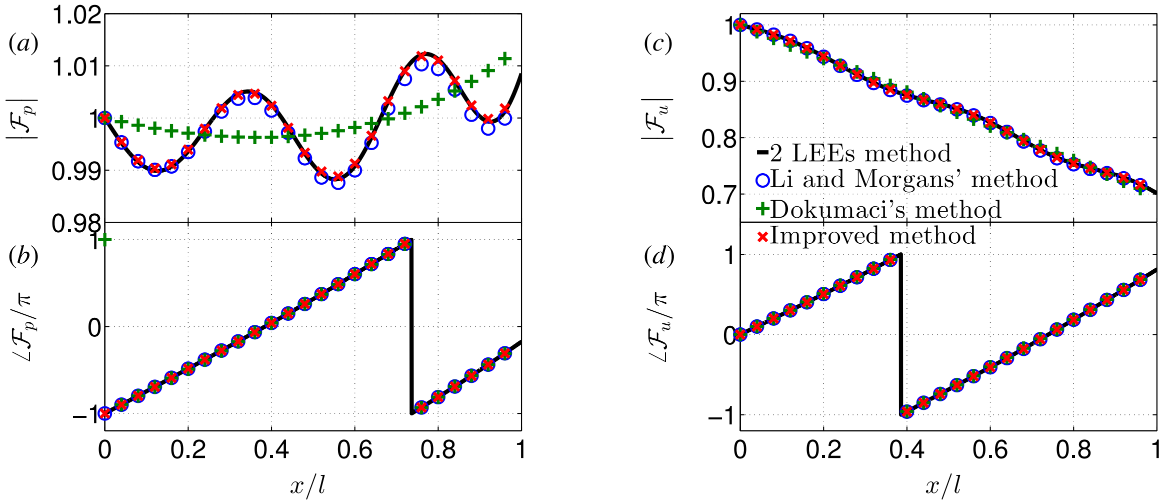


Figure 2: Evolution of $\mathcal{F}_p$ and $\mathcal{F}_u$ with $x$ for the linear mean temperature profile. $\overline{T}_1 = 1600$ K, $\overline{T}_2 = 800$ K, $M_1 = 0.2$. $fl/\bar{c}_1 = 1$. $Z_1 = -1$. (a): transfer function gain $|\mathcal{F}_p|$. (b): transfer function phase $\angle\mathcal{F}_p$. (c): transfer function gain $|\mathcal{F}_u|$. (d): transfer function phase $\angle\mathcal{F}_u$.

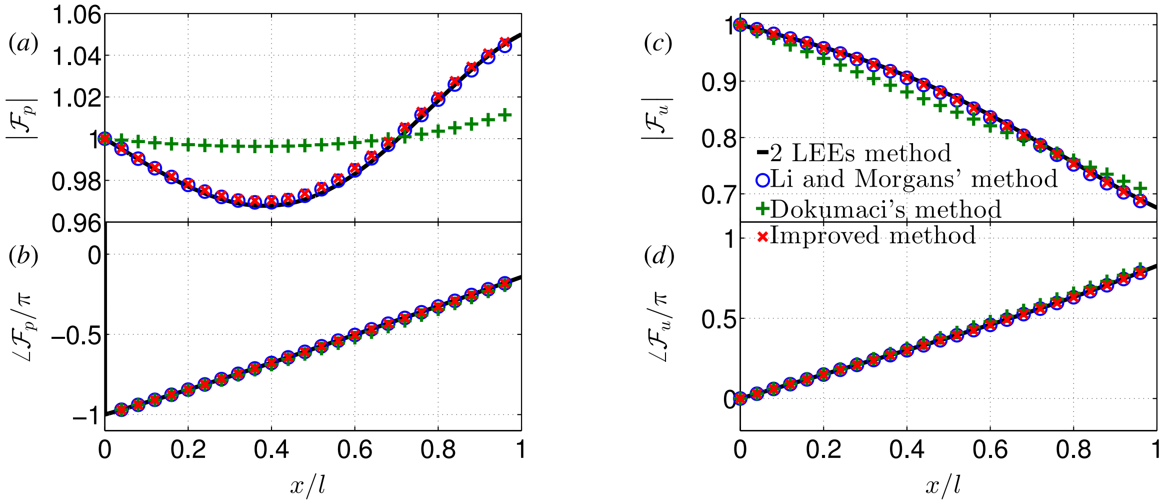


Figure 3: Evolution of $\mathcal{F}_p$ and $\mathcal{F}_u$ with $x$ for the linear mean temperature profile. $\overline{T}_1 = 1600$ K, $\overline{T}_2 = 800$ K, $M_1 = 0.2$. $fl/\bar{c}_1 = 0.3$. $Z_1 = -1$. (a): transfer function gain $|\mathcal{F}_p|$. (b): transfer function phase $\angle\mathcal{F}_p$. (c): transfer function gain $|\mathcal{F}_u|$. (d): transfer function phase $\angle\mathcal{F}_u$.

It is interesting to note that this exactly matches Eq. (47) in [3]. To the authors' knowledge, the improved analytical solution given by Eqs. (3) and (5) generally has higher accuracy than Eqs. (3) and (4) of Dokumaci's comment, particularly at lower frequencies. The criterion pertaining to this improved analytical solution follows from the method in Dokumaci's previous research [2] (pages 857-858). Equations accounting for mean flow, rather than neglecting it, are used to derive the criterion, which approximately equals that of our previous analytical solution [3]. Figures 1-3 confirm that performance of our improved analytical solution is better than both our previous solution and Dokumaci's.

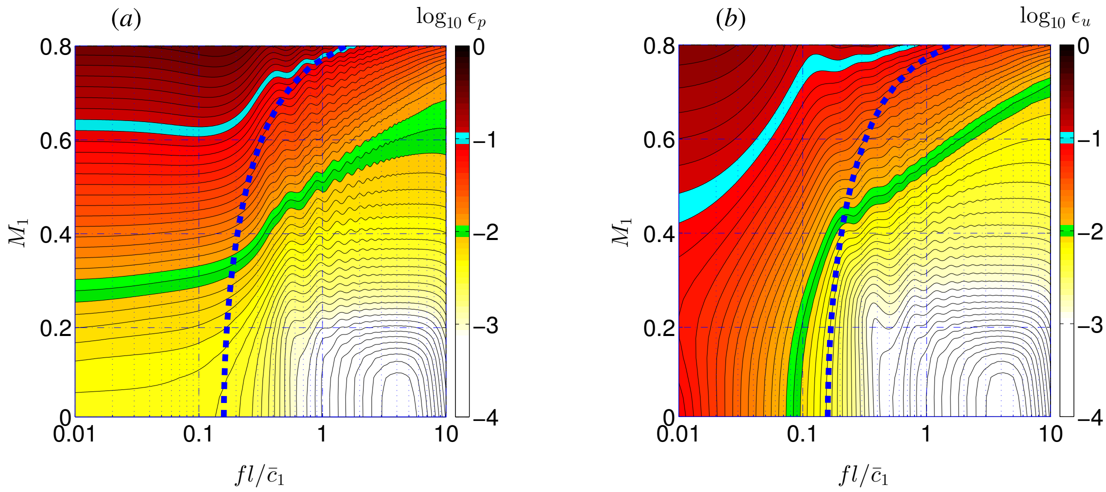


Figure 4: Contour maps of (a) $\epsilon_p$ and (b) $\epsilon_u$ using our previous analytical solution as functions of $fl/\bar{c}_1$ and $M_1$ for the linear mean temperature profile. The dashed line represents $\chi$ as a function of $M_1$. $\overline{T}_1 = 1600$ K, $\overline{T}_2 = 800$ K and $Z_1 = -1$.

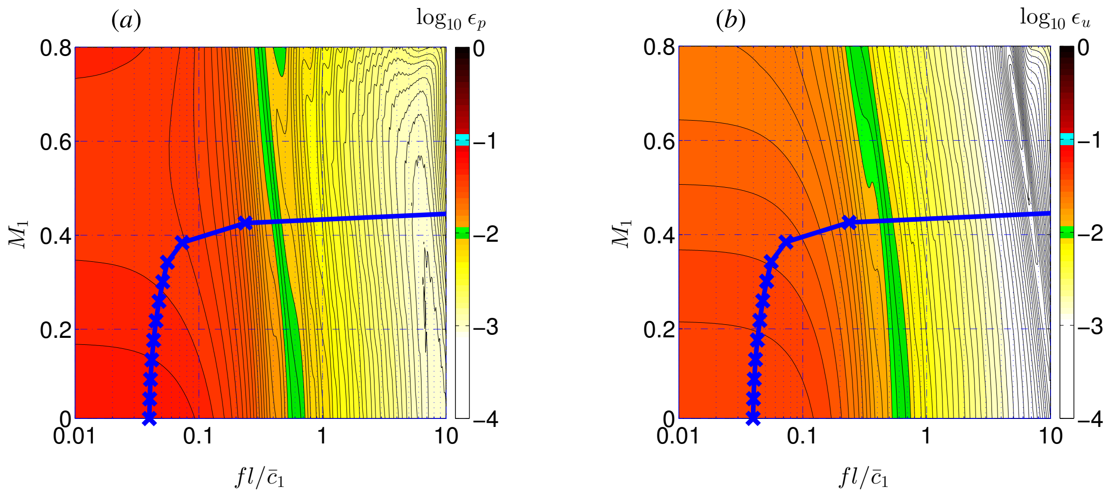


Figure 5: Contour maps of (a) $\epsilon_p$ and (b) $\epsilon_u$ using the Dokumaci's solution as functions of $fl/\bar{c}_1$ and $M_1$ for the linear mean temperature profile. Markers $\times$ represent $\chi_d$ as a function of $M_1$. $\overline{T}_1 = 1600$ K, $\overline{T}_2 = 800$ K and $Z_1 = -1$.

## 3. Validation

### *3.1. Linear axial temperature variation*

As in our previous work [3], a parametric study provides further insights into the accuracy of the three analytical solutions across different frequencies, $fl/\bar{c}_1$, Mach numbers, $M_1$, and temperature ratios, $\overline{T}_2/\overline{T}_1$. Figures 4 - 9 show the error coefficients, $\epsilon_p$ and $\epsilon_u$ (defined in Eqs. (58) and (59) in [3]), for analytical solutions obtained using our previous method (Figs. 4 and 7), Dokumaci's solution (Figs. 5 and 8) and our improved solution (Figs. 6 and 9).

For moderate Mach numbers (e.g. $M_1 < 0.4$) our previous solution maintains high accuracy across all reduced frequencies, while Dokumaci's solution performs well only at higher frequencies. It is interesting to note that Dokumaci's solution has a better performance when both the inlet Mach number, $M_1$, and the reduced frequency are large. Dokumaci's frequency criterion (Eq. (8) in his comment, with representation of $\psi$ given by Eqs. (8) and (9)) is plotted,

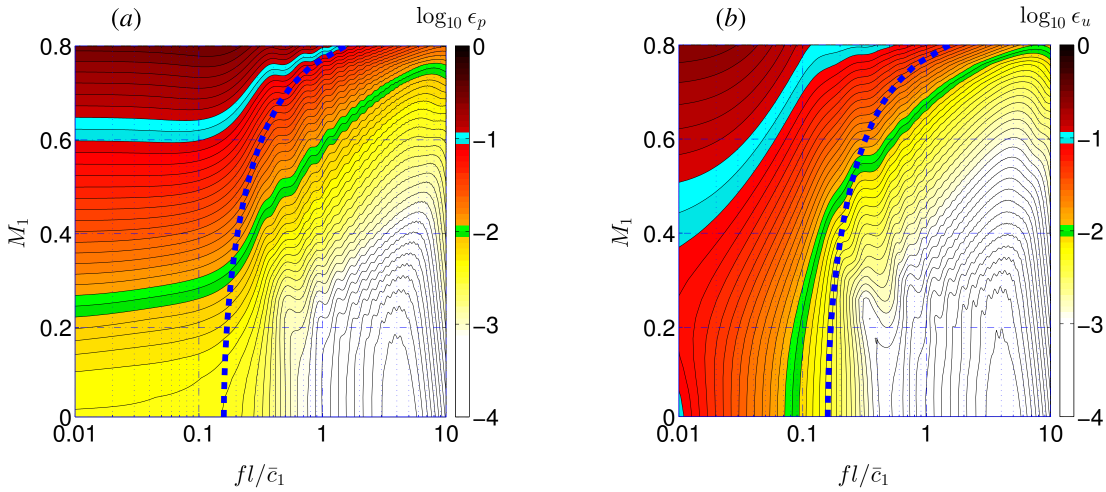


Figure 6: Contour maps of (a) $\epsilon_p$ and (b) $\epsilon_u$ using the improved analytical solution as functions of $fl/\bar{c}_1$ and $M_1$ for the linear mean temperature profile. The dashed line represents $\chi$ as a function of $M_1$. $\overline{T}_1 = 1600$ K, $\overline{T}_2 = 800$ K and $Z_1 = -1$.

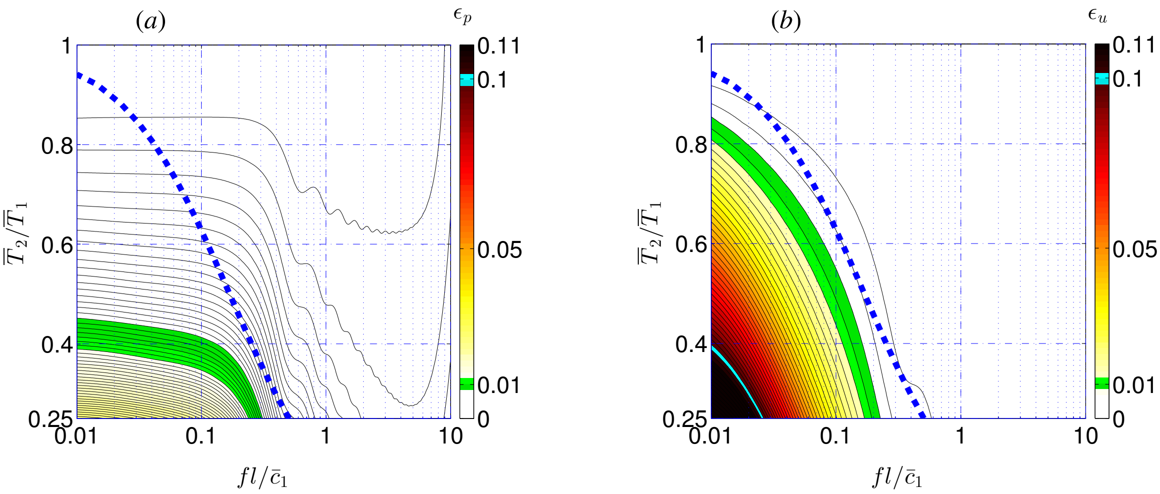


Figure 7: Contour maps of (a) $\epsilon_p$ and (b) $\epsilon_u$ using our previous solution as functions of $fl/\bar{c}_1$ and $\overline{T}_2/\overline{T}_1$ for the linear mean temperature profile. The dashed line represents $\chi$ as a function of $\overline{T}_2/\overline{T}_1$. $\overline{T}_1 = 1600$ K, $M_1 = 0.2$ and $Z_1 = -1$.

given by:

$$\frac{fl}{\bar{c}_1} \gg \chi_d = \frac{l}{2\pi\bar{c}_1}\left(\max\left(\bar{c}^2\left|\psi\frac{\mathrm{d}}{\mathrm{d}x}(\ln\bar{c}) + \frac{\mathrm{d}\psi}{\mathrm{d}x}\right|, \frac{\bar{c}^2}{4}\left|2\psi\frac{\mathrm{d}}{\mathrm{d}x}(\ln\bar{c}) + 2\frac{\mathrm{d}\psi}{\mathrm{d}x} + \psi^2\right|\right)\right)^{\frac{1}{2}} \tag{6}$$

Fig. 5 shows that the criterion is only satisfied at smaller Mach numbers, with the performance of the solution only good when the reduced frequency significantly exceeds this criterion.

Our improved solution combines the advantages of our previous solution and Dokumaci's solution; it reproduces the acoustic field accurately even at low frequency, larger Mach number conditions.

### 3.2. *Sine-wave axial temperature variation*

The performance of the three analytical solutions, for sine-wave axial mean temperature profiles (full details given in [3]), are shown in Figures 10 - 12. Predictions by applying our previous solution in a piecewise linear manner are

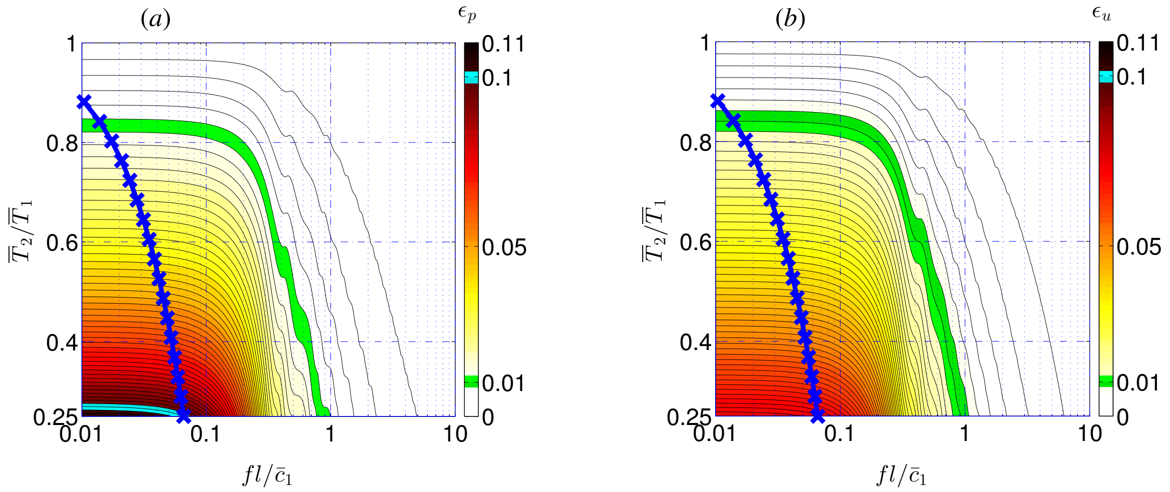


Figure 8: Contour maps of (a) $\epsilon_p$ and (b) $\epsilon_u$ using Dokumaci's solution as functions of $fl/\bar{c}_1$ and $\overline{T}_2/\overline{T}_1$ for the linear mean temperature profile. Markers × represent $\chi_d$ as a function of $\overline{T}_2/\overline{T}_1$. $\overline{T}_1 = 1600$ K, $M_1 = 0.2$ and $Z_1 = -1$.

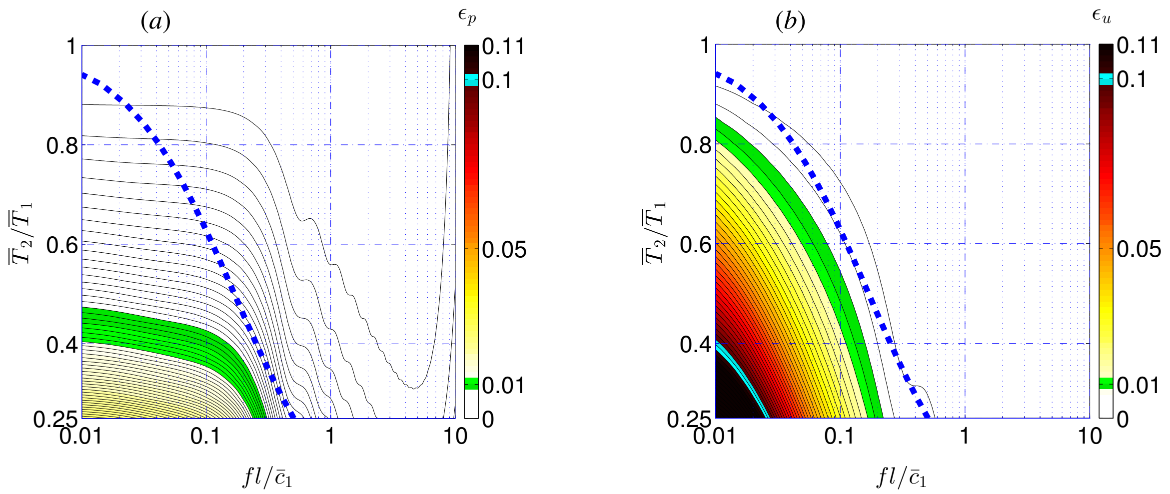


Figure 9: Contour maps of (a) $\epsilon_p$ and (b) $\epsilon_u$ using our improved solution as functions of $fl/\bar{c}_1$ and $\overline{T}_2/\overline{T}_1$ for the linear mean temperature profile. The dashed line represents $\chi$ as a function of $\overline{T}_2/\overline{T}_1$. $\overline{T}_1 = 1600$ K, $M_1 = 0.2$ and $Z_1 = -1$.

also shown, using $N_s = 40$ axial segments. At very low Mach numbers and relatively large frequencies, all of the analytical predictions capture the acoustic field accurately. As the Mach number, $M_1$, increases, the predicted acoustic fields from the three versions of our analytical solution remain good, while predictions using Dokumaci's solution exhibit inaccuracies. At lower reduced acoustic frequency, $fl/\bar{c}_1$, our previous solution, current improved solution and Dokumaci's solution, when applied globally to the temperature field, are not able to reproduce the acoustic field; only the piecewise linear approach yields accurate predictions of the acoustic field.

## Conclusions

Our previous and improved analytical solutions for the one-dimensional acoustic field in a duct with an axial mean temperature gradient and mean flow generally apply over a wider frequency range than Dokumaci's solution. As Mach

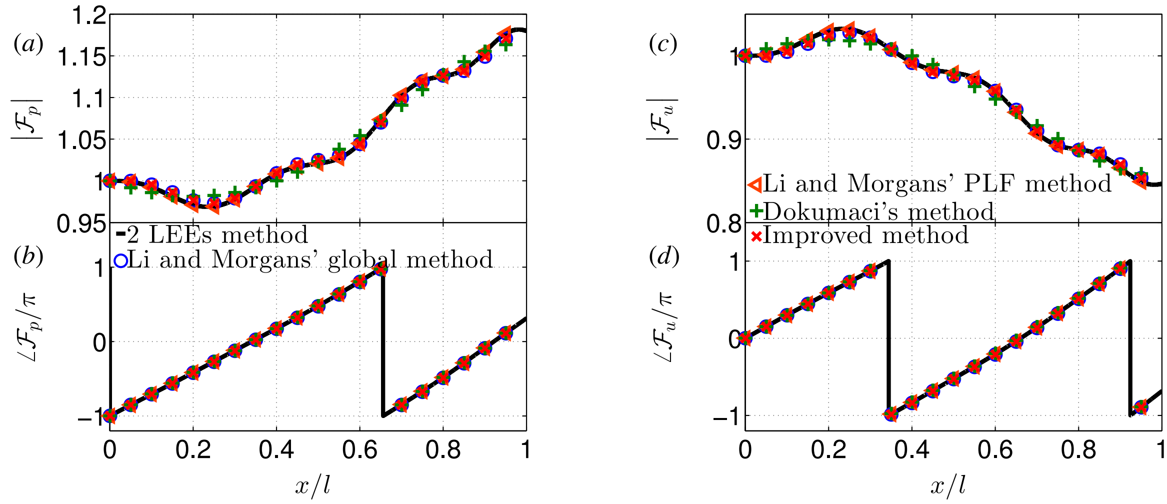


Figure 10: Evolution of $\mathcal{F}_p$ and $\mathcal{F}_u$ with $x$ for the sine mean temperature profile. $\overline{T}_1 = 1600$ K, $\overline{T}_2 = 800$ K, $M_1 = 0.001$, $fl/\bar{c}_1 = 1.5$ and $Z_1 = -1$. (a): transfer function gain $|\mathcal{F}_p|$. (b): transfer function phase $\angle\mathcal{F}_p$. (c): transfer function gain $|\mathcal{F}_u|$. (d): transfer function phase $\angle\mathcal{F}_u$.

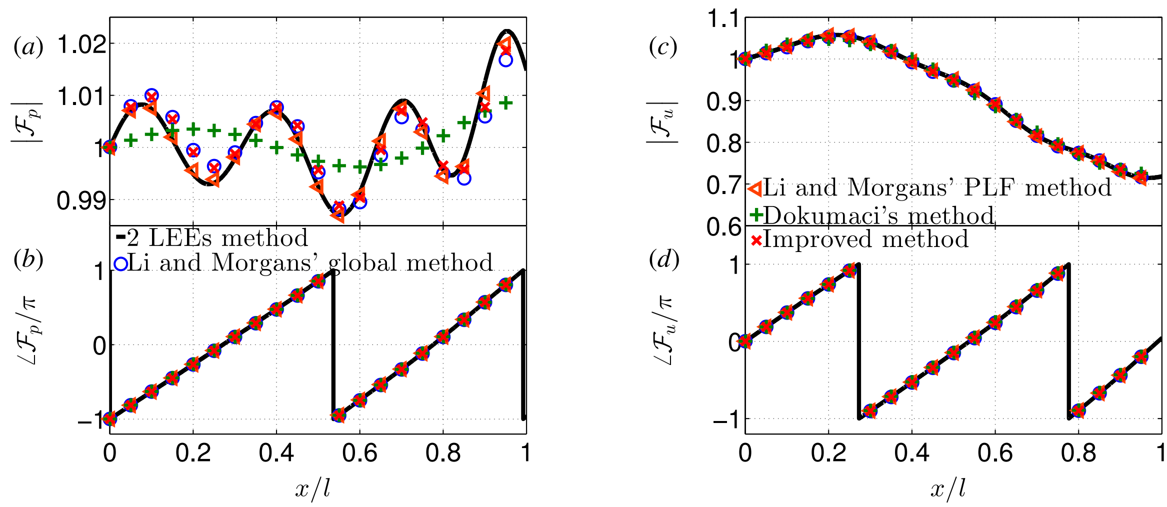


Figure 11: Evolution of $\mathcal{F}_p$ and $\mathcal{F}_u$ with $x$ for the sine mean temperature profile. $\overline{T}_1 = 1600$ K, $\overline{T}_2 = 800$ K, $M_1 = 0.2$. $fl/\bar{c}_1 = 1.5$. $Z_1 = -1$. (a): transfer function gain $|\mathcal{F}_p|$. (b): transfer function phase $\angle\mathcal{F}_p$. (c): transfer function gain $|\mathcal{F}_u|$. (d): transfer function phase $\angle\mathcal{F}_u$.

number terms with higher orders are retained in the diagonal terms of the matrizant, his solution can be used for larger Mach number flow conditions as long as the frequency is sufficiently large. The frequency criterion of Dokumaci's solution is derived by neglecting mean flow, while those for our previous and improved solutions account for mean flow, and so it would not be rigorous to conclude that his criterion is tighter than ours. Finally, it should be noted that our previous analytical solution only needs thermodynamic and mean flow properties at the beginning and end of the region with mean temperature distribution, while Dokumaci's and our improved solutions need the properties in the entire region, meaning that our previous solution is easier to use.

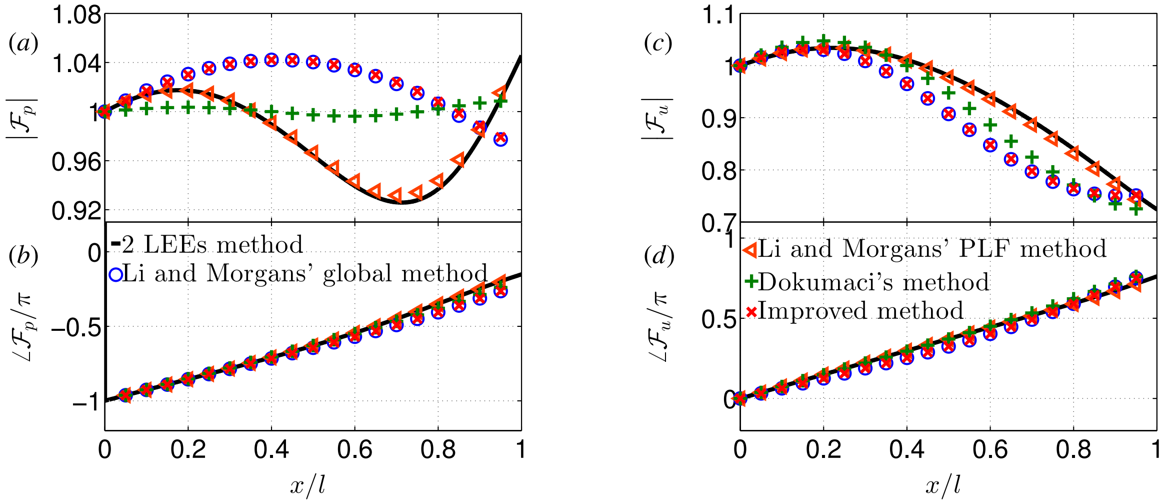


Figure 12: Evolution of $\mathcal{F}_p$ and $\mathcal{F}_u$ with $x$ for the sine mean temperature profile. $\overline{T}_1 = 1600$ K, $\overline{T}_2 = 800$ K, $M_1 = 0.2$. $fl/\bar{c}_1 = 0.3$. $Z_1 = -1$. (a): transfer function gain $|\mathcal{F}_p|$. (b): transfer function phase $\angle\mathcal{F}_p$. (c): transfer function gain $|\mathcal{F}_u|$. (d): transfer function phase $\angle\mathcal{F}_u$.

## Acknowledgement

The authors would like to gratefully acknowledge the European Research Council (ERC) Starting Grant (grant no.305410) ACOULOMODE (2013-2018) for supporting the current research.

## References

[1] E. Dokumaci, Transmission of sound in uniform pipes carrying hot gas flows, *J. Sound Vib.* 195 (1996) 257–266.

[2] E. Dokumaci, An approximate analytical solution for plane sound wave transmission in inhomogeneous ducts , *J. Sound Vib.* 217 (1998) 853–867.

[3] J. Li, A. S. Morgans, The one-dimensional acoustic field in a duct with arbitrary mean axial temperature gradient and mean flow, *J. Sound Vib.* 400 (2017) 248–269.